Reduced and oxidized rice straw biochar for hexavalent chromium adsorption: Revisiting the mechanism of adsorption

Amarjeet Dahiya [a], Akanksha Bhardwaj [b], Archana Rani [a], Meenu Arora [c], J. Nagendra Babu [a],*

[a] *Department of Chemistry, School of Basic Sciences, Central University of Punjab, VPO Ghudda, Badal Road, Punjab, 151401, India*
[b] *Department of Environmental Science & Technology, Central University of Punjab, VPO Ghudda, Badal Road, Bathinda, Punjab, 151401, India*
[c] *Department of Chemistry, Maharaja Ranjit Singh Punjab Technical University, Badal Road, Bathinda, Punjab, 151001, India*

ARTICLE INFO

ABSTRACT

Surface oxygen functional groups of biochar were tuned by oxidation and reduction of biochar for establishing Cr(VI) adsorption mechanism. Oxygen functional groups (OFGs) on the surface of leached rice straw biochar (LBC4-6) obtained from pyrolysis at 400, 500 and 600 °C, were oxidized to furnish OBC4-6 using modified Hummer's method. Reduced biochar RBC4-6 were obtained by esterification and $NaBH_4/I_2$ reduction of oxidized biochar (OBC4-6). The modified biochar were characterized by increase in O/C and H/C ratio, respectively, in case of OBC4-6 and RBC4-6. The Cr(VI) adsorption by modified biochar LBC4-6, OBC4-6, and RBC4-6 showed optimum conditions of pH 3 and dose 0.1 g/L with a good non-linear fit for Langmuir & Freundlich isotherm. The maximum adsorption (Q_m) followed the trend: OBC4 (17.47 mg/g) > RBC4 (15.23) > OBC5 (13.23) > LBC4 (10.23) > RBC5 (9.83) > OBC6 (9.60) > RBC6 (7.24) > LBC5 (6.32) > LBC6 (5.98). The adsorption kinetics for adsorption of Cr(VI) on to modified biochar fits pseudo second order (PSO), Elovich and intraparticle diffusion kinetics, showing a chemisorptions in case of biochar L/O/RBC4-6. The lower temperature modified biochar O/RBC4 show better Cr(VI) adsorption. X-ray Photoelectron Spectroscopy (XPS) studies establish optimum OFGs for reduction of Cr(VI) and chelation of the reduced Cr(III). Adsorption and stripping cycles show the oxidized and reduced biochar as better adsorbents with excellent stripping of Cr up to >98 % upon desorption with 1 M NaOH.

1. Introduction

Increase in heavy metal in environment is attributed to industrialisation and improper hazardous waste management. Cr is one of the most commonly found heavy metal pollutant in environment. Various anthropogenic sources including tannery, electroplating, smelting, agriculture, construction and electronic manufacturing [1] contribute for Cr in our environment. Cr exists as hexavalent chromium (Cr(VI)) and trivalent chromium (Cr(III)) in the water bodies. Chromium contaminated water bodies pose a significant threat to human health, as exposure to chromium can result in various adverse health effects [2]. Remediation of Cr is a major challenge due to its high toxicity and persistence in the environment. Cr(III) is an essential nutrient for plants and animals, while Cr(VI)

Abbreviation

Cr(VI)   Hexavalent Chromium
TCLP   Toxicity Characteristic Leaching Procedure
LBC4-6   Leached BioChar pyrolyzed at 400, 500 and 600 °C temperature
OBC4-6   Oxidized BioChar pyrolyzed at 400, 500 and 600 °C temperature
RBC4-6   Reduced BioChar pyrolyzed at 400, 500 and 600 °C temperature
FT-IR   Fourier Transform InfraRed
FESEM   Field Emission Scanning Electron Microscopy
BET   Brunauer–Emmett–Teller
BJH   Barrett–Joyner–Halenda
XPS   X-ray Photoelectron Spectroscopy

---

is highly toxic, mutagenic, and carcinogenic [3–5]. Treatment and removal of Cr from water/wastewater is carried out using techniques namely, chemical precipitation [6], reverse osmosis [7], electrocoagulation [8], nanofiltration [9], bioremediation [10], membrane separation [11], and (ad)sorption [12–14]. However, these techniques have significant drawbacks, including incomplete removal of Cr(VI), poor selectivity & scalability, high costs & energy consumption, sludge waste and adaptability in industrial setup. On the other hand, adsorption is a surface technology, wherein chromium would be retained on the solid surface of the adsorbents and separated from the wastewater. Adsorption is a relatively cost-effective, low-energy process that is easy to implement, acceptable as technology for treatment of water [15]. Thus, adsorptive removal of Cr from various process wastewaters using cheaper adsorbents including biosorbents (biomass) [16], municipal wastes, sewage sludge [17] and pig manure [18], apart from activated carbon [19] and fly ash [20], have been studied.

Biochar is a term broadly applied to carbon-rich material obtained from the pyrolysis of organic wastes, such as biomass, manure, sludge [21]. Biochar from various source show versatile properties which make its usage in carbon sequestration and storage [22], supercapacitors [23], energy catalysis [24], and adsorption [25]. Biochar from various wastes have been studied for adsorption of heavy metals [26], and organic contaminants [27], due to the existence of various modes of interaction of adsorbate on biochar surface including electrostatic, hydrogen bonding, ion-dipole, dipole-dipole, pi-pi interaction, London forces, etc. The chromium adsorption on biochar takes place by Cr(VI) reduction by surface oxidation of either oxygen functional groups (OFGs) [28], or Persistent Free Radical (PFRs) [29]. The PFRs on biochar surface were studied for Cr(VI) reductive adsorption [30] which upon exposure to sunlight increase the Cr(VI) adsorption in the presence of quinoid functional moieties on the surface of the adsorbent. The interfacial surface transfer of electron is through an indirect reduction using the radical oxygen system (ROS) O$_2$, HO· [31], etc. produced at the interface of the solid and bulk liquid followed by Cr(VI) reduction and adsorption of Cr(III)/Cr(VI) ions. Due to ill-defined interaction between biochar and Cr(VI), biochar are poor adsorbents for Cr(VI) adsorption. Rice straw biochar in particular are poor adsorbent of Cr(VI) in comparison to biochar obtained from other biomass substrates [32]. Rice straw biochar has limited use as adsorbent due to significant silica content, needs promotion for carbon neutral agricultural sustainable development in developing countries [33]. Cr(VI) adsorption using biochar has been improved by either surface activation or modification of biochar surface covalently or non-covalently i.e., surface functionalization or composite formation with inorganic/organic materials. The surface area and access to surface functional moieties are improved by pre and post-pyrolytic activation with acids (H$_3$PO$_4$, ZnCl$_2$) and bases (NaOH, KOH, K$_2$CO$_3$) for Cr(VI) adsorption on modified biochar [34]. The biochar functionalized with organic moieties like pre-pyrolysis co-doping with N/S [35], and post-pyrolytic co-doping using ethylene diamine [36], chitosan [37], polyaniline [38] etc, improve the positive surfaces charge at lower pH, improving hydrogen bonding and electrostatic interaction [39]. BiWO$_6$ [35] and TiO$_2$ [40] as inorganic modifiers on the surface of biochar tend to improve the adsorption of Cr(VI) by photochemical reduction with adsorption. There has been no significant study on the use of oxidized or reduced biochar for improving the Cr(VI) adsorption by reduction of adsorbate.

Thus, in continuation of our findings on Cr(VI) remediation by redox mechanism using biomass [16], fly ash [20] and composites [41,42], it is proposed that the surface oxidation and reduction, respectively, of biochar would improve OFGs and reduced OFGs (alcohol and phenol), furnishing adsorbent with improved Cr(VI) adsorption. The oxidized biochar would improve oxidized OFGs including carboxylic acids, carbonyl/quinone/semiquinone, phenols and epoxide, which could improve the PFR and chelation based mechanism [43]. One the contrary, the reduced biochar prepared from dense OFG containing oxidized biochar, will lead to reduction based Cr(VI) adsorption. Thus, establishing the influence of oxidized and reduced OFGs on Cr(VI) adsorption confirming mechanism on biochar surface.

2. Results and discussion

2.1. Characterization of LBC4-6, OBC4-6 and RBC4-6

Synthesis of oxidized and reduced biochar was carried out as depicted in Scheme 1. In brief, the leached biochar was oxidized by modified Hummer's method using KMnO$_4$, H$_2$SO$_4$/H$_3$PO$_4$ (9:1, v/v) oxidation followed by H$_2$O$_2$ treatment [41] to furnish OBC4-6. The oxidized biochar OBC4-6 was subjected to esterification using methanol/HCl followed by reduction with NaBH$_4$/I$_2$ in THF suspension to furnish the reduced biochar RBC4-6 (Scheme 1).

The synthesized biochar O/RBC4-6 were characterized by various proximate and ultimate analysis as given in Table 1. The ultimate analysis of the leached, oxidized and reduced biochar L/O/RBC4-6 reveals significant change in the stoichiometry of the C, O and H upon synthetic modifications (Table 1). The atomic ratio O/C was improved upon oxidation of LBC4-6 to OBC4-6, whereas H/C deteriorates, which is accounted to the surface oxidation of biochar OBC4-6. Similarly, reduced biochar RBC4-6 show improved H/C ratio, which is accounted to the reduction of OFGs in RBC4-6. The pH of the biochar L/O/RBC4-6 corroborates with the oxidation followed by reduction of the functional moieties on surface. The oxidized biochar OBC4-6 are generally acidic in nature due to surface oxidation which produces acidic functional group including sulphonates and carboxylates [42]. pH of modified biochar LBC4-6 and OBC4-6 lie in range 1.63–2.05 whereas biochar RBC4-6 is neutral to slightly basic i.e., 7.0–8.0, which corroborate with the reduction of acidic functional moieties to neutral functional groups like primary/secondary/tertiary alcohols and phenols in case of biochar RBC4-6.

FESEM images reveal the surface morphology and porosity characteristics of the biochar surface [42]. The surface morphology of OBC4 and RBC4 is depicted as given in Fig. 1 a-b. The biochar OBC4 showed smaller particles of biochar in comparison to biochar LBC4. Further, the images reveal an increased porosity of biochar OBC4 in comparison to LBC4. This decrease in particle size and increase in the porosity of biochar OBC4 could be attributed to the oxidation of skeletal carbon leading to particle breakup and porosity. Similarly, biochar RBC4 show a closure of pores and smoother surface upon reduction with borohydride solution which precipitates Na$^+$ ions and other coordinating organic moieties.

The surface functional group change upon redox modification of biochar was monitored using FTIR spectroscopy (Fig. S1). A broad peak was observed at wavelength 3284.65 cm^{-1} for biochar OBC4, attributed to O–H stretching vibration (Fig. 1c). Similarly, the O–H stretching bands were observed at 3304.05 and 3291.31 cm^{-1}, respectively, for LBC4 and RBC4. Absorption band corresponding to the carbonyl and carboxylate functional moieties were observed at 1744.70, 1718.27 and 1741.48 cm^{-1}, respectively for biochar LBC4, OBC4 and RBC4. The C=C stretching peaks of L/O/RBC4 were observed at 1622.21, 1609.96, and 1618.99 cm^{-1}, respectively. Adsorption band at 1089.69 cm^{-1} observed in case of OBC4 is attributed to lactone or ester C–O stretching vibration [44,45]. Upon adsorption of Cr(VI) on the biochar L/O/RBC4, the C=C stretching bands were shifted to 1596.42, 1621.57 and 1601.58 cm^{-1}, respectively [46,47].

The surface charge of biochar L/O/RBC4-6 was monitored by the zeta potential of biochar as a function of pH (Fig. 1 d-f). Biochar L/O/RBC4-6 showed negative potential in the pH range of 2–12, which is attributed to increased deprotonation of surface functional groups [48,49]. The surface oxidized and reduced biochar O/RBC4-6 showed similar zeta potential at various pH [50]. However, at pH 4–10, biochar OBC4-6 showed a lowering of surface charge due to the protonation of the carbonyl/quinone moiety [51]. The biochar RBC4-6 show an increase in negative zeta potential with pH, attributed to the deprotonation of reduced alcohol/phenols in reduced biochar under basic conditions [52].

The surface area and pore distribution characteristics of the biochar L/O/RBC4-6 is as given in Table 1. The N$_2$ adsorption–desorption isotherm behaviour of the modified biochar show a BET type IV isotherm with a H3-hysteresis loop indicating mesoporous structure being intact throughout the oxidation as well as reduction of biochar [53]. However, there is a significant increase in the surface area ascribed to pore development upon mineralization of carbon in case of oxidized biochar OBC4-6 [54,55]. The pore diameter and volumetric distribution were analyzed for the biochar L/O/RBC4-6, as depicted in Fig. 1g-i. The pore diameter and pore volume of oxidized biochar OBC4-6 showed a decrease and increase, respectively, in comparison to leached biochar LBC4-6. This could be attributed to the carbon mineralization in case of OBC4-6. However, the pore diameter increased in case of the biochar RBC4-6 due to the blockage of the smaller pores in OBC4 upon reduction. These findings corroborate with that observed in SEM images of biochar L/O/RBC4-6.

2.1.1. XPS spectra

XPS studies reveal the change in surface OFGs on biochar upon oxidation followed by reduction for modified biochar L/O/RBC4. The full survey scan of L/O/RBC4 showed negligible changes, with the C1s and O1s spectra observed at ∼292 and ∼584 eV, respectively in case of modified biochar L/O/RBC4 (Fig. S2). Deconvolution of the C1s and O1s peaks were studied for the speciation
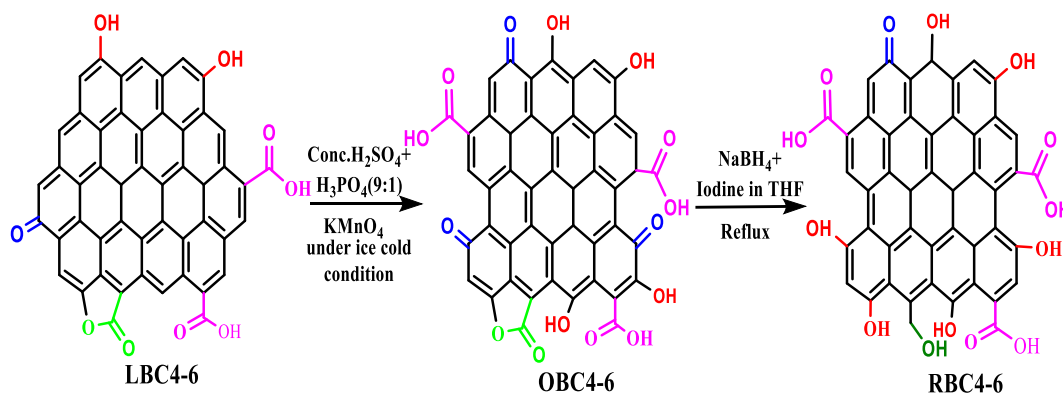
Scheme 1. Synthesis of oxidized (OBC4-6) and reduced biochar (RBC4-6).

Table 1
Physio-chemical and surface characteristics of Leached and modified rice straw biochar (L/O/RBC4-6).

	LBC4	LBC5	LBC6	OBC4	OBC5	OBC6	RBC4	RBC5	RBC6
pH	5.41	5.36	5.00	1.63	1.84	2.05	7.44	7.63	8.90
C (%)	49.76	39.56	56.35	47.48	58.56	54.36	45.83	54.3	61.56
H (%)	5.139	4.536	2.472	3.067	2.516	1.941	3.256	2.409	2.054
N (%)	0.28	0.25	0.46	8.23	8.18	8.75	8.95	9.07	9.42
S (%)	0.46	0.23	0.28	2.516	1.556	0.257	1.217	0.587	0.481
O (%)	19.921	28.684	12.558	16.887	4.548	8.292	16.107	9.034	9.34
H/C ratio	1.239	1.376	0.526	0.775	0.516	0.428	0.853	0.532	0.40
O/C ratio	0.300	0.544	0.167	0.392	0.160	0.229	0.405	0.247	0.108
Ash Content (in %)	24.44 ± 0.028	26.74 ± 0.042	27.88 ± 0.042	21.82 ± 0.049	24.64 ± 0.057	26.40 ± 0.064	24.64 ± 0.049	24.60 ± 0.049	26.56 ± 0.010
Volatile content (in %)	72.20 ± 0.078	57.48 ± 0.057	57.20 ± 0.127	70.00 ± 0.085	61.40 ± 0.106	52.04 ± 0.113	74.72 ± 0.098	68.84 ± 0.537	65.84 ± 0.093
Fixed Carbon content	3.36 ± 0.064	15.78 ± 0.078	14.92 ± 0.156	8.18 ± 0.216	13.96 ± 0.092	21.56 ± 0.112	0.66 ± 0.120	6.76 ± 0.106	7.60 ± 0.077
Moisture Content (in %)	6.43 ± 0.059	6.48 ± 0.037	6.80 ± 0.064	11.42 ± 0.051	7.84 ± 0.091	7.28 ± 0.049	14.14 ± 0.134	9.22 ± 0.118	7.23 ± 0.043
Surface Area ($m^2 g^{-1}$)	6.033	9.159	79.045	8.574	24.353	30.765	7.379	12.671	12.502
Average Pore Diameter (nm)	26.816	20.739	4.682	14.525	6.534	9.603	15.734	15.234	19.521
Pore Volume (BJH) (V_p) ($cm^3 g^{-1}$)	0.0588	0.054	0.1045	0.0332	0.0793	0.0677	0.0265	0.0321	0.0516

dynamics during chemical transformation and adsorption using the modified biochar L/O/RBC4 (Fig. 2 a-f). Deconvolution of C1s peak of LBC4 revealed four major peaks at 283.53 (3.39 %), 284.02 (35.24 %), 284.66 (39.81 %), 286.24 (21.56 %) and a minor peak at about ~288 eV, accounted to the presence of C–C (graphite skeleton), C–O(alcoholic/phenolic), C═O (ketone/aldehyde), carboxylate and lactones, respectively [42]. A shift in the deconvoluted C1s peaks was observed in case of OBC4 in comparison to LBC4. The C1s peaks for biochar OBC4 were observed at 284.33 (28.69 %), 285.06 (33.29 %), 286.23 (18.99 %) and 288.65 (19.02 %) eV, which could be accounted to the C–O, C═O, carboxylate and lactones, respectively. These results show a significant loss of graphitic skeleton on the surface of biochar OBC4, which is attributed to the mineralization of carbon upon oxidation of LBC4. Further the peak observed at 288.65 eV is significant, accounted to oxidation of biochar OBC4 leading to OFGs undergoing lactone cyclization under acidic conditions of reaction [41]. The deconvoluted C1s peak with an increase in the peak area for unsaturated OFGs likes C═O and COO, respectively, at 285.06 and 286.23 eV. Further deconvoluted O1s peaks at 530.97 (14.00 %), 531.85 (23.61 %), 532.59 (34.39 %) and 533.33 (28.05 %) eV, are attributed to Inorganic-O, OH, COOH, COO^- ions, respectively, whereas in case of OBC4, they deconvolute at 531.47 (12.14 %), 532.27 (23.84 %), 532.94 (33.95 %) and 533.67 (28.0 %) eV, respectively. There is a significant increase in carboxylate oxygen with loss of C–OH [56]. Thus, the XPS studies confirm the oxidation of LBC4 surface to yield oxidized biochar OBC4.

Reduced biochar RBC4 showed a significant change in the XPS spectra as compared to OBC4. The C1s deconvoluted peaks of RBC4 at 283.99 (28.23 %), 284.63 (34.73 %), 285.82 (21.92 %) and 288.04 (15.11 %) eV, respectively for C–OH, C═O, COO and lactone functional groups (Fig. 2c). The results show a significant decrease in the C1s peak area at 288.04 and 285.82eV, whereas peak at 284.63 eV, show a marginal decrease, which could be attributed to the existence of epoxide/carbonyl groups which have tendency to get reduced, in comparison to carboxylic and lactone moieties. Thus, reduction of OBC4 with a decrease in carboxylic functional group and increase in the phenolic/alcoholic moieties observed in reduced biochar RBC4.

Upon Cr(VI) adsorption onto biochar OBC4, deconvoluted C1s peak were observed at 284.33 (27.49 %), 285.04 (38.96 %), 286.23 (20.62 %) and 288.65 (12.93 %) eV, respectively, characteristic of C–OH, C═O, COO and lactone (Fig. 3a). The deconvoluted peaks due to Cr(VI)-OBC4, a significant change in the peak area upon Cr(VI) adsorption. There is an increase in the area under the C1s peak at 285.04 eV and 286.23 eV, whereas the area under the peak at 284.33 eV showed a decrease. These changes in the C1s peak is attributed to the oxidation of the C–OH functional groups to carbonyl and carboxylate functional groups during the adsorption of Cr(VI) using OBC4.The high resolution Cr2p spectra of Cr-adsorbed OBC4 are as shown in Fig. 3c. The peaks corresponding to $Cr2p_{3/2}$ and $Cr2p_{1/2}$ were visible at 577.98 and 587.92 eV, respectively. Upon deconvolution three pair of peaks at (577.52, 587.19), (578.38, 581.85), and (571.46, 573.87) eV, for ($Cr2p_{3/2}$, $Cr2p_{1/2}$) are characteristic of Cr(VI), Cr(III) and Cr^0, respectively. Thus, the oxidation of biochar OBC4 in presence of Cr(VI) is evident from the presence of Cr(III) and Cr^0 in Cr-sorbed OBC4. Resonate changes were observed in case of O1s peaks which showed high resolution peaks at 531.47, 532.31, 533.05 and 533.83 eV (Fig. 3b). Upon comparison with the O1s peaks of OBC4, significant decrease in the peak area for O1s peak of C–O–H peak at 532.31 eV, with an increase in the peak area at 533.05 and 533.83 eV were observed. These changes corroborate with the adsorption of Cr(VI) onto biochar OBC4, which takes place with the reduction of Cr(VI) to Cr(III) ions followed by adsorption of Cr(III) ions by favourable ion-exchange phenomenon. Meanwhile, the carbon skeleton of biochar underwent oxidation to carboxylic acid and carbonyl group in Cr adsorbed OBC4 [57].
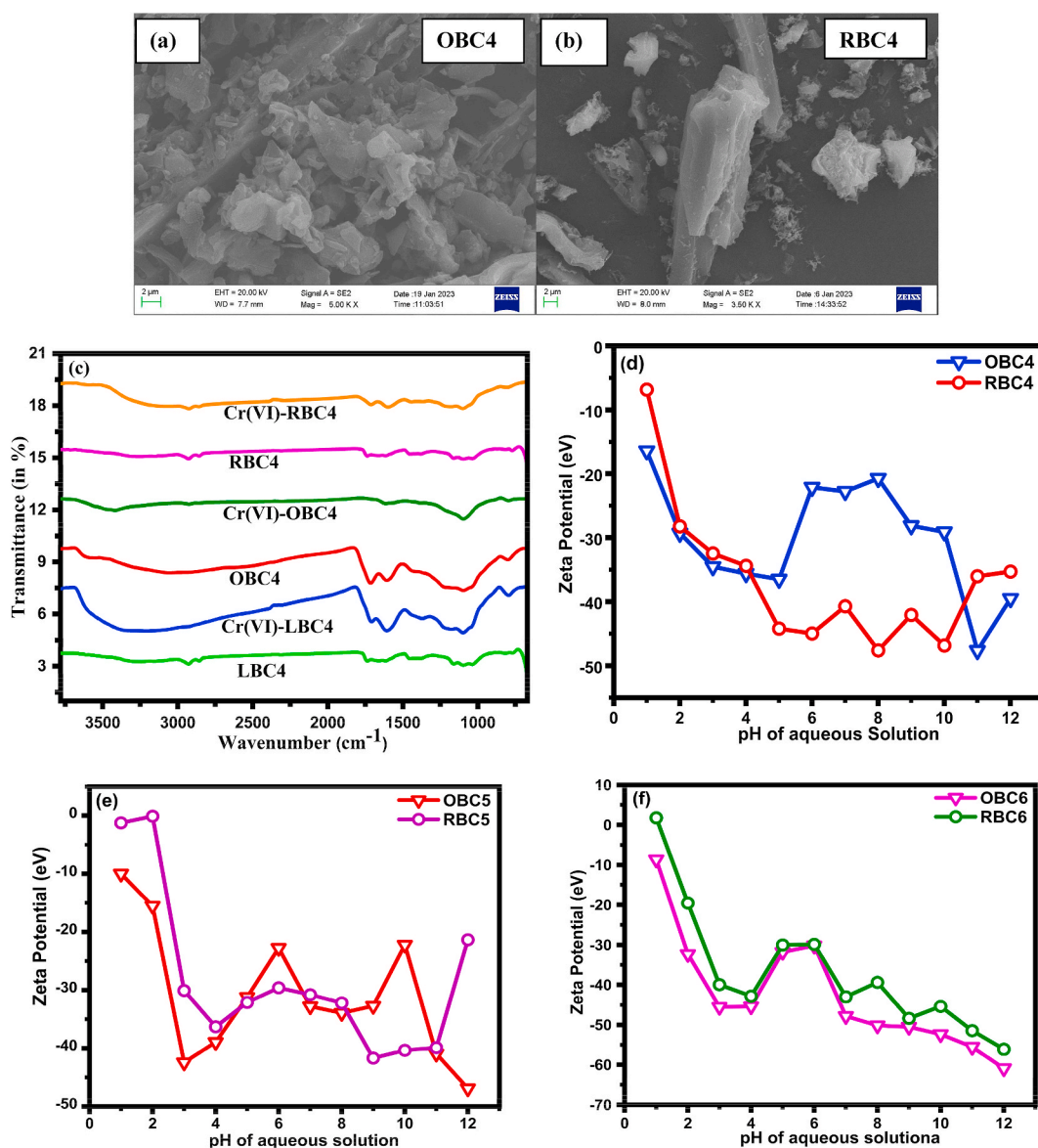
Fig. 1. Physicochemical characteristics of oxidized and reduced biochar: SEM images of **(a)** OBC4;**(b)** RBC4;**(c)** FTIR spectra of L/O/RBC4 and Cr (VI) adsorbed L/O/RBC4; Zeta potential of **(d)** O/RBC4 **(e)** O/RBC5 and **(f)** O/RBC6; BET adsorption-desorption curve of **(g)** OBC4-6, **(h)** RBC4-6; and **(i)** corresponding volumetric pore size distribution BJH Plot for L/O/RBC4.

2.2. Adsorption studies and isotherms

2.2.1. Effect of pH on Cr(VI)

The pH of solution plays a vital role in speciation and adsorption of chromate ion in aqueous solution. Thus, to study the effect of initial pH on Cr(VI) removal, adsorption studies were performed in the pH range of 3–10 with adsorbent dose of 0.1 g/L using 10 mg/L Cr(VI) solution for 24 h (Fig. 4a). For the biochar L/O/RBC4-6, the Cr(VI) uptake efficiency decreased as pH increased from 3 to 10, with maximum adsorption observed at pH 3. The Q_e for Cr(VI) adsorption on biochar LBC4-6, OBC4-6 and RBC4-6 are respectively, 7.50, 5.31 and 5.78; 16.55, 12.65 and 6.25; 13.28, 9.37, and 6.56 mg/g. Adsorption of Cr(VI) on L/O/RBC4 decreased with increase in initial pH of Cr(VI) aqueous solution from 3 to 10 as 9.06 to 3.59, 19.83 to 7.65 and 22.80 to 0.16 mg/g, respectively.The higher removal efficiency for Cr(VI) at lower pH is ascribed to (a) surface protonation of biochar O/RBC4-6, resulting in lowering of negative charge on surface, and protonation of chromate ions ($HCrO_4^-$), which reduces electrostatic repulsion between protonated chromate and the surface of modified biochar [58,59].Under acidic pH reduction of Cr(VI) is also favoured. At higher pH, Cr(VI) exists as a dianion (CrO_4^{2-}) and deprotonated carboxylate surface of O/RBC4-6 are both unfavourable for electrostatic interaction leading to poor electron
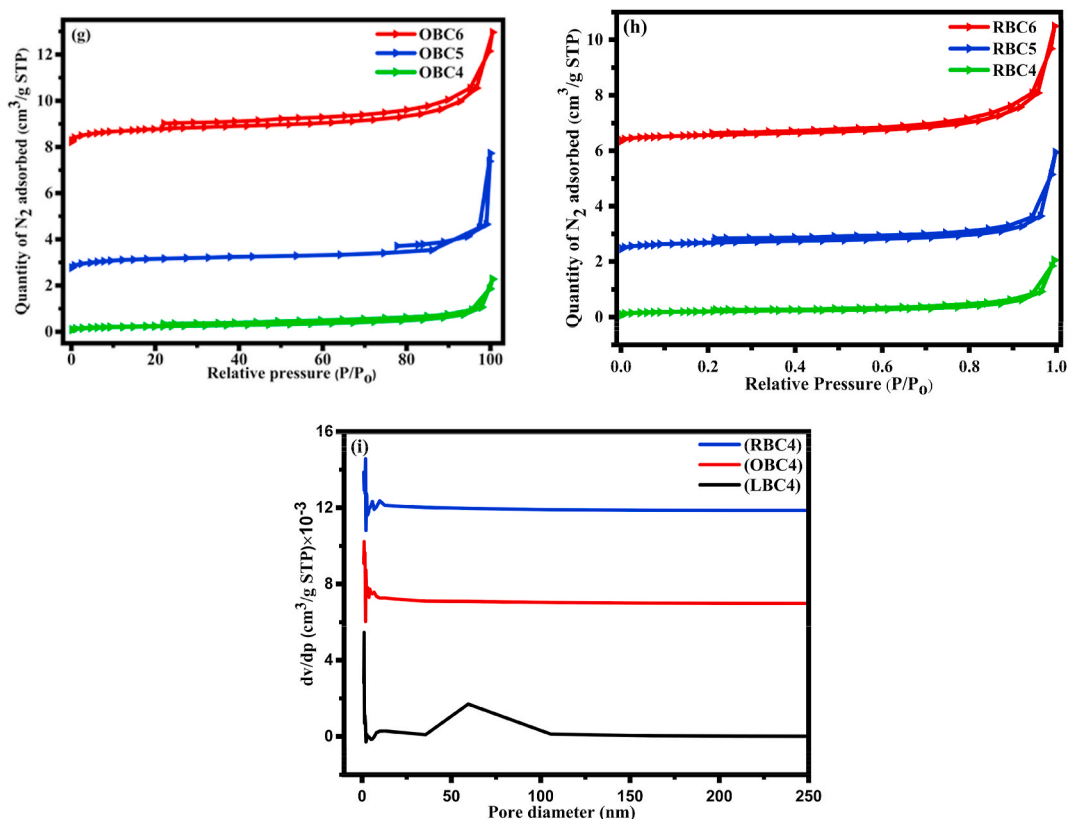
Fig. 1. (*continued*).

transfer as well as adsorption [47,58].

2.2.2. Effect of LBC4-6, OBC4-6 and RBC4-6 dose on Cr(VI) adsorption

Effect of biochar L/O/RBC4 dose on Cr(VI) adsorption were investigated by varying the amount of adsorbent from 0.05 to 0.20 g/L using 10 mg/L aqueous Cr(VI) solution maintained at pH 3 (Fig. 4b). As the adsorbent dose of L/O/RBC4 increased from 0.05 to 0.20 g/L, the Cr(VI) removal increased from 5 to 11 %, 10–34 %, and 8–32 %, respectively. This increase in removal efficiency of L/O/RBC4 with dosage could be attributed to the increase in the number of available reactive/adsorptive sites on biochar with increase in adsorbent dosage [60]. Similarly, with an increase in the adsorbent dose, the adsorption efficiency (Q_e) showed an optimum at 14.21, 20.93 and 20.14 mg/g, respectively for L/O/RBC4 at 0.1 g/L dosage (Fig. 4b). There is marginal decrease in the adsorption efficiency upon increasing the dose which could be attributed to increase in number of pores is not linear with the increase in adsorbent dose i.e., there is an increase in adsorbent collision which result in this disproportionate behavior [61].

2.2.3. Effect of initial Cr(VI) concentration on adsorption by LBC4–6, OBC4-6, and RBC4-6 and adsorption isotherms

Cr(VI) uptake equilibrium was investigated by varying initial concentration of aqueous Cr(VI) solution from 2 to 10 mg/L maintained at pH 3, adsorbent dose of 0.1 g/L and contact time of 24 h (Fig. 4c–e). The removal of Cr(VI) decreased with increase in initial Cr(VI) concentration from 13.24 to 7.88, 12.06 to 5.58 and 11.38 to 6.08 %, respectively, for leached biochar LBC4, LBC5 and LBC6.The increase in the number of Cr(VI) with increase in initial concentration, compete for same quantity of available active sites on the adsorbent thus leading to decrease in Cr(VI) removal upon adsorption using LBC4-6 [62]. Similar trend of decrease in Cr(VI) removal efficiency with increase in initial concentration of Cr(VI) was observed in case of oxidized and reduced biochar O/RBC4-6. However, in case of oxidized and reduced biochar (O/RBC4-6), the Cr(VI) removal efficiency were atleast three-fold higher than that of the LBC4-6. This clearly indicates that oxidized and reduced biochar have conducive environment on their surface for adsorption of Cr(VI). In case of oxidized biochar, the adsorption efficiency (Q_e) were17.47, 13.23 and 9.60 mg/g, respectively for modified biochar OBC4, OBC5 and OBC6. The Cr(VI) adsorption efficiency (Q_e) was 15.26, 9.54 and 7.24 mg/g, respectively, for RBC4, RBC5 and RBC6. OBC4-6 and RBC4-6 show similar adsorption of Cr(VI) ions, thus indicating a common mechanism underlying the interaction of the Cr(VI) with the surface of modified biochar.

Further insight into the type of interactions between the adsorbent and adsorbate is obtained by fitting the equilibrium Cr(VI) concentration to non-linear Langmuir [63] and Freundlich adsorption isotherm fit were studied (Fig. 5).The non-linear form of Langmuir isotherm (Eq. (1)) is given as follows
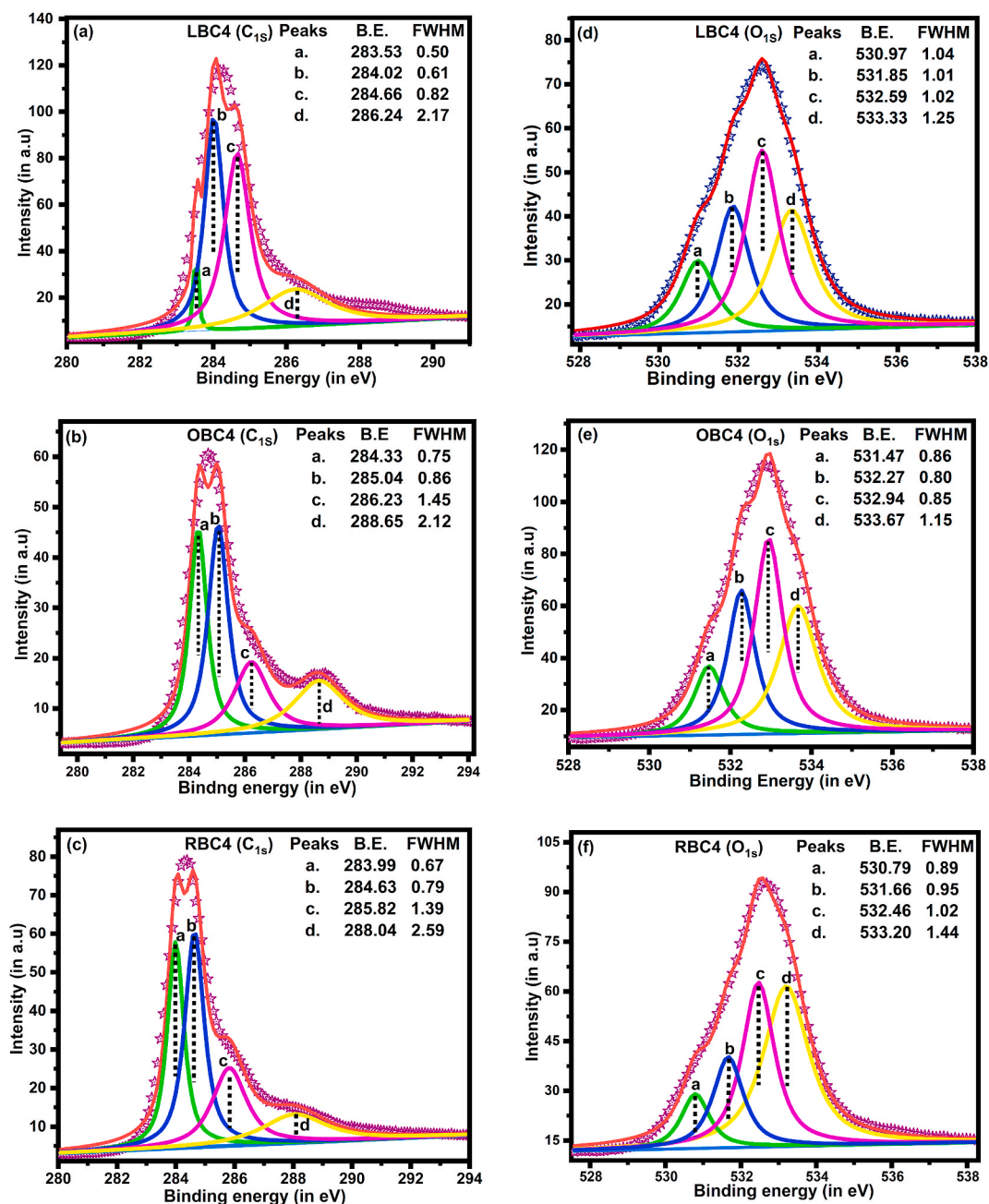
Fig. 2. XPS studies of L/O/RBC4 (a), (b), and (c) for C$_{1s}$, and (d), (e), and (f) for O$_{1s}$ XPS studies High resolution X-ray photoelectron spectra of leached biochar and modified biochar.

$$Q_e = \frac{C_e Q_m K_L}{1 + K_L C_e} \tag{1}$$

where Q$_m$ is the maximum adsorption capacity (mg/g), C$_e$ is equilibrium Cr(VI) concentration (mg/L), Q$_e$ is amount of Cr(VI) adsorbed under equilibrium(mg/g) and K$_L$ is Langmuir constant (L/mg). The maximum adsorption capacity (Q$_m$) obtained from Langmuir model (Table 2), for modified biochar can be arranged in decreasing order as OBC4 (17.47 mg/g) > RBC4 (15.23 > OBC5 (13.23) > LBC4 (10.23) > RBC5 (9.83) > OBC6 (9.60) > RBC6 (7.24) > LBC5 (6.32) > LBC6 (5.98 mg/g). This trends suggests the Cr(VI) adsorption was poor in case of LBC4-6 (Fig. 5a) in comparison to OBC4-6 (Fig. 5b), and RBC4-6 (Fig. 5c), which could be accounted to the increased abundance of oxygen functional moieties in O/RBC4-6. Freundlich isotherm [64] on the other hand assumes multi-layer coverage on adsorbent heterogeneous surface. The non-linear form of this model (Eq. (2)) is expressed as follows-
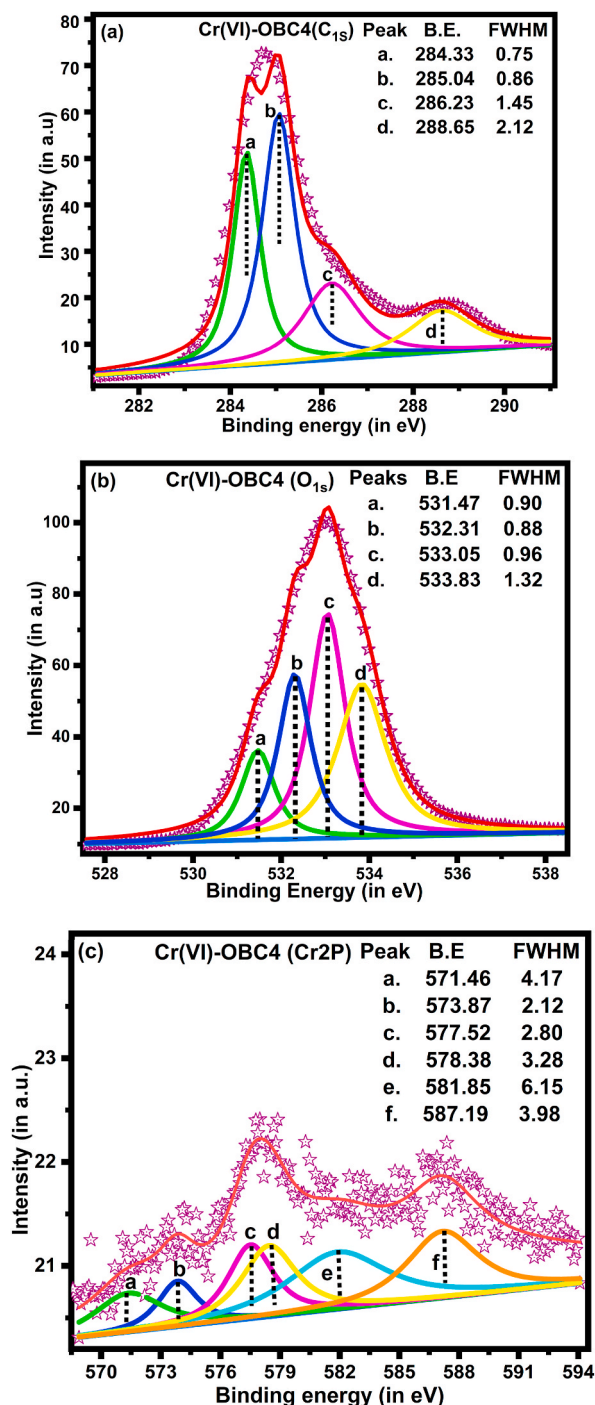
Fig. 3. XPS studies of Cr(VI)-adsorbed by OBC4; **(a)** C_{1s}, **(b)** O_{1s} and **(c)** Cr_{2p}, X-ray photoelectron spectra of oxidized biochar (OBC4) after Cr (VI)-adsorption.

$$Q_e = K_F C_e^{\frac{1}{n}} \tag{2}$$

where K_F is Freundlich constant related to adsorption capacity and n is related to adsorption intensity. If the value of $1/n < 1$, the adsorption is spontaneous and cooperative. In the present study, the value of $1/n$ for all the biochar were in the range of 0–1, which signifies spontaneous Cr(VI) adsorption on the modified biochar L/O/RBC4-6 [65]. The Cr(VI) adsorption using modified biochar L/O/RBC4-6 showed a better fit with Freundlich model compared to Langmuir model as inferred from the R^2 values for both the
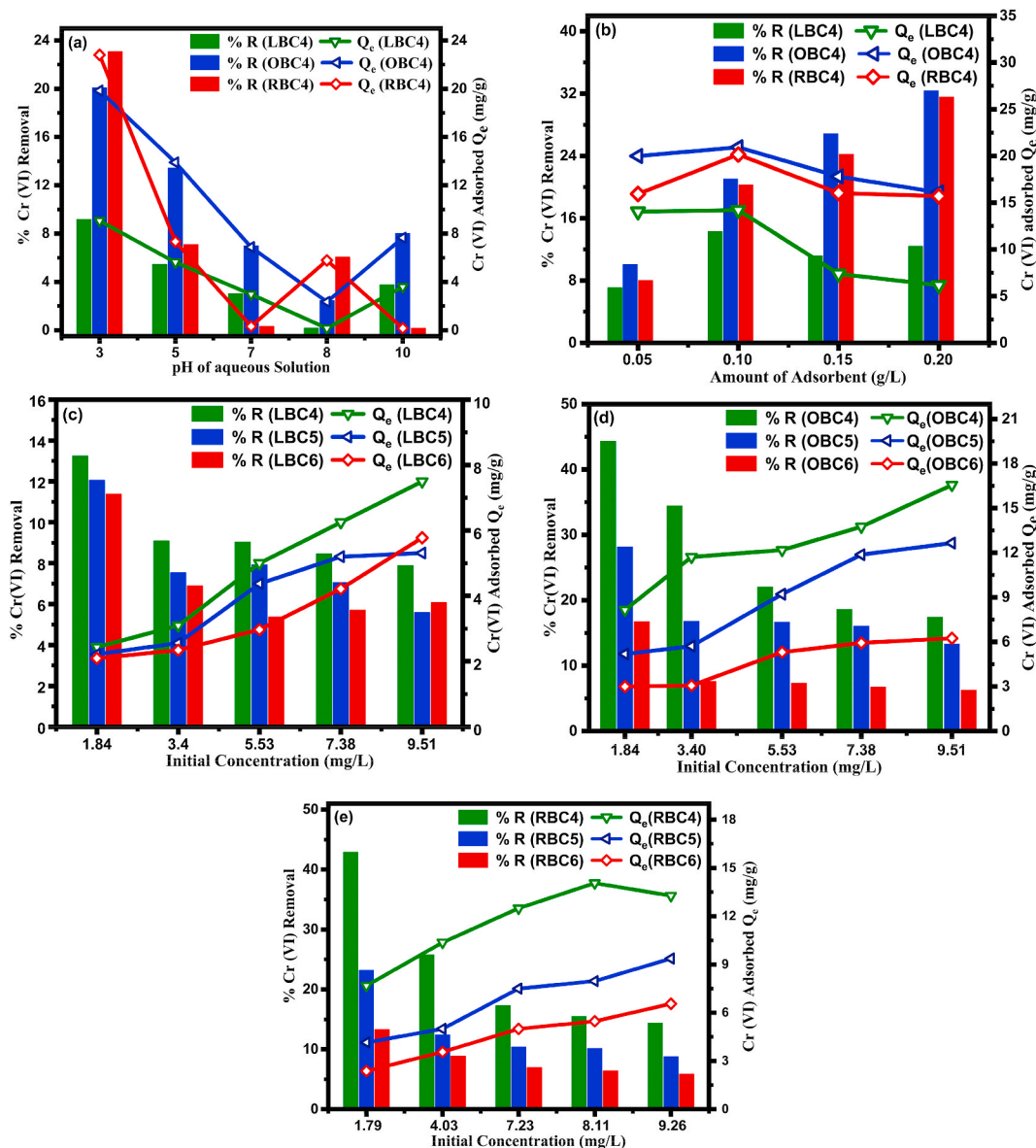
Fig. 4. (a). Effect of pH 3–10 on Cr(VI) (0.01 g/L) removal; **(b).** Effect of adsorbent dose on (0.05–0.20 g/L) Cr(VI) (0.01 g/L) removal by L/O/RBC4; and **(c–e).** Effect of initial Cr(VI) concentration (2–10 mg/L) adsorption by LBC4-6, OBC4-6, and RBC4-6 (LBC4-6 = Leached biochar 400, 500, and 600.

models (Table 2), which is consistent with a lognormal decrease in heat of adsorption with occupancy on the surface of adsorbent.

2.2.4. Effect of contact time and kinetic model analysis

The effect of contact time on Cr(VI) removal using modified biochar L/O/RBC4, was studied for time ranging from 0 to 24 h at pH 3, biochar dosage of 0.1 g/L and initial Cr(VI) concentration 0.01 g/L (Fig. 6 a-c). The removal of Cr(VI) increased with contact time in case of all the biochar. The Cr(VI) adsorption onto biochar increased up to 14.6, 21.6 and 19.5 %, respectively for LBC4 (Fig. 6a), OBC4 (Fig. 6b) and RBC4 (Fig. 6c) within 7 h of equilibrium. Non-linear fitting of the kinetic behavior for Cr(VI) adsorption using L/O/RBC4 was studied by Pseudo first order (PFO) (Eq. (3)), Pseudo second order (PSO) [66] (Eq. (4)), Intraparticle Diffusion (IPD) [36] (Eq. (5)), liquid film diffusion (LFD) [67] (Eq. (6)), and Elovich [13] (Eq. (7)) as follows:

$$\text{Pseudo first order (PFO)} \quad Q_t = Q_e \left(1 - e^{-kt}\right) \tag{3}$$

$$\text{Pseudo second order (PSO)} \quad Q_t = \frac{k_t Q_e^2 t}{1 + k_t Q_e t} \tag{4}$$
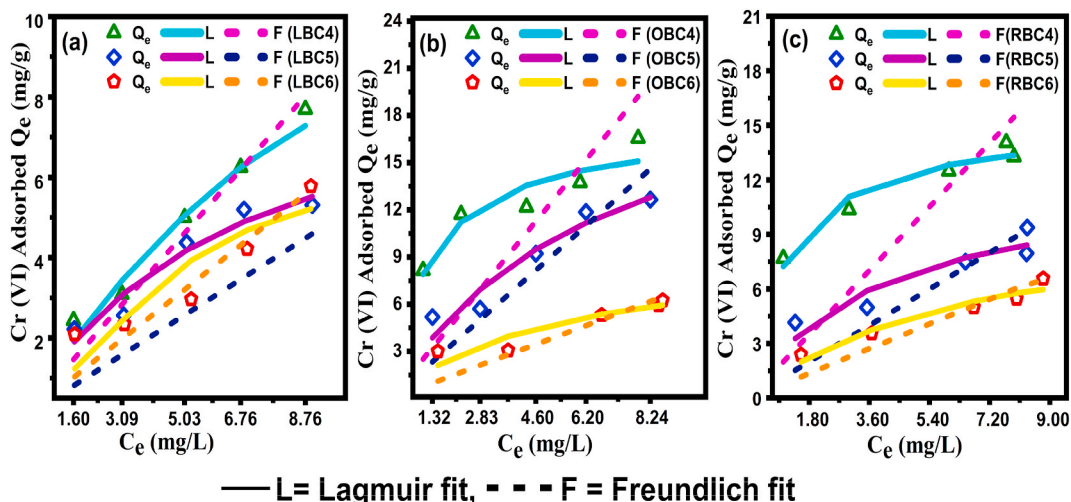
Fig. 5. Non-linear regression fit of Langmuir and Freundlich adsorption isotherm model for Cr(VI) adsorption by **(a).** LBC4-6, **(b).** OBC4-6, and **(c).** RBC4-6.

Table 2
Langmuir and Freundlich isotherm characteristics of LBC4-6, OBC4-6 and RBC4-6 for Chromium [Cr(VI)] adsorption.

Adsorbent	Langmuir isotherm				Freundlich isotherm			
	Q_{max} (mg/g)	K_L (L/mg)	R^2	SSE	K_F (L/mg))	n	R^2	SSE
LBC4	10.23	0.206	0.972	1.762	1.490	1.625	0.995	1.453
LBC5	6.32	0.997	0.928	1.461	1.152	2.252	0.919	0.585
LBC6	5.98	0.308	0.867	2.859	1.216	1.907	0.964	1.406
OBC4	17.47	0.807	0.933	4.911	8.184	3.343	0.956	81.743
OBC5	13.23	0.524	0.923	11.559	3.565	2.012	0.970	14.318
OBC6	9.60	0.189	0.919	1.692	1.917	2.557	0.968	3.938
RBC4	15.27	0.882	0.974	1.368	7.279	3.736	0.979	59.323
RBC5	9.83	0.542	0.906	3.743	2.995	2.696	0.967	9.747
RBC6	7.24	0.361	0.949	1.571	1.387	1.835	0.985	2.408

Q_m is the maximum adsorption capacity (mg/g); K_L is Langmuir constant (L/mg); K_F is Freundlich constant related to adsorption capacity; **n** is related to adsorption intensity.
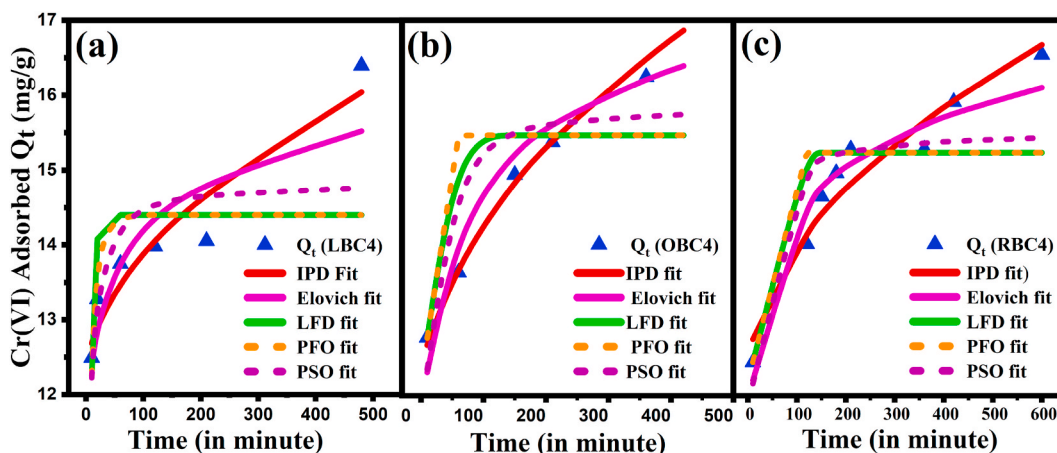
Fig. 6. Intra-particle diffusion (**IPD**), Elovich, Liquid film diffusion (**LFD**), Pseudo- first order (**PFO**), and Pseudo-second order (**PSO**) model fitting plots of Cr (VI) removal for (a–c) initial concentration (0.01 g/L) of Cr (VI) using leached and modified biochar (a) LBC4, (b) OBC4, and (c) RBC4.

$$\text{Intraparticle diffusion (IPD)} \mathbf{Q_t} = \mathbf{k_p} \sqrt{\mathbf{t}} + \mathbf{C} \tag{5}$$

$$\text{Liquid film diffusion (LFD)} \mathbf{Q_t} = \mathbf{Q_e} \left(1 - \mathbf{e}^{-\mathbf{k_{fd}}\,\mathbf{t}}\right) \tag{6}$$

$$\text{Elovich equation} \mathbf{Q_t} = \boldsymbol{\beta} \ln \boldsymbol{\alpha\beta} + \boldsymbol{\beta} \ln \mathbf{t} \tag{7}$$

Where, Q_e (mg/g) and Q_t (mg/g) are the amounts of adsorbate uptake per mass of adsorbent at equilibrium and at any time t (min), respectively, and k_1 (min^{-1}); K_2 (g/mg min); k_p (mg/g min$^{1/2}$); k_{fd} (min^{-1}); is the rate constant of the PFO, PSO, IPD, and LFD equation and C is a constant for any experiment (mg/g) referring to characteristic of boundary layer for IPD equation. Whereas α (mg min^{-1}) is the initial removal rate; β (g mg^{-1}) is a constant associated with surface coverage and activation energy for Elovich equation and R_e is Elovich equilibrium parameter, where Elovich equilibrium parameter is given as $\mathbf{R_e} = \boldsymbol{\beta}/\mathbf{Q_e}$.

The results showed that the PSO, IPD and Elovich model showed better fit for adsorption of Cr(VI) onto L/O/RBC4 with the Q_e closer to Q_m (obtained from Langmuir isotherm fit) (Table 3). The PSO rate constant for Cr(VI) adsorption on biochar LBC4, OBC4 and RBC4 were respectively, 3.17×10^{-2}, 1.12×10^{-2} and 6.81×10^{-3} g/mg min^{-1}, which show a strong concentration dependence of adsorption in case of OBC4 and RBC4 in comparison to LBC4. PSO and Elovich model fit indicates the chemisorption of Cr(VI) onto the adsorbent biochar [68,69]. The desorption parameter (b) was found to be more in case of modified biochar OBC4 and RBC4, in comparison to LBC4. The Elovich equilibrium parameter (Re) for LBC4 and OBC4 is found to lie between 0.3 and 0.02, which indicates type II mild rising curves [70]. Intraparticle diffusion fit showed an intercept which closely resembled the maximum adsorption, followed by the diffusion characteristics inside the biochar.

3. Regeneration studies

Leached, oxidized, and reduced biochar L/O/RBC4 was used in batch desorption studies for Cr(VI) (Fig. 7). In equilibrium at pH 3, for a 24 h contact time, 0.5 g/L of L/O/RBC4 was added to 10 mg/L of Cr(VI) solution to furnish saturated Cr(VI)-adsorbed L/O/RBC4. The Cr(VI)-adsorbed LBC4 obtained was studied for desorption characteristics with 1 M NaOH, 1 M HCl, and methanol, as stripping agents [42]. The initial adsorption of Cr(VI) was 8.51, 13.18 and 8.96 mg/g observed for L/O/R BC4 during the first adsorption cycle. Upon desorption with 1 M NaOH, 1 M HCl or methanol and stripping time of 1 h, a maximum desorption based recovery was observed for Cr(VI) using 1 M NaOH as stripping agent up to 3.26, 2.25 and 0.99 mg/g, respectively for biochar LBC4. Thus desorption of the OBC4 and LBC4 was carried out in 1 M NaOH and furnish quantitative Cr recovery of >98 %. The improved desorption in case of oxidized and reduced biochar (O/RBC4) is attributed to the ion-exchangeable Cr(III) on the surface of these biochar. The biochar L/O/RBC4 regenerated from the first cycle of adsorption-desorption, showed poor adsorption in the second cycle with adsorption of 5.70, 6.31 and 5.22 mg/g which is attributed to the destruction of the pore during the alkali treatment.

Table 3
Non-linear fit of adsorption kinetics for Cr(VI) removal by leached and modified biochar.

		LBC4	OBC4	RBC4
PFO	Q_e (mg/g) calculated	14.40	21.243	18.630
	K_1 (h^{-1})	0.190	0.148	0.099
	R^2	0.614	0.683	0.789
	SSE	5.417	22.420	24.913
PSO	Qe (mg/g) (calculated)	14.830	21.946	19.350
	K_2 (g/mg h)	0.032	0.011	0.0068
	R^2	0.753	0.790	0.852
	SSE	3.826	15.688	18.399
IPDM	K_{ipd} (mg/g h$^{1/2}$)	0.179	0.435	0.456
	C_1 (mg/g)	12.120	14.840	11.03
	R^2	0.960	0.994	0.970
	SSE	0.792	0.523	3.939
Elovich	a (mg/g h)	5.47×10^5	141.115	4.713
	β (g/mg)	0.809	1.964	2.359
	R^2	0.896	0.948	0.965
	SSE	1.705	4.203	4.521
LFDM	Q_e (mg/g)	14.401	21.242	18.629
	K_{fd}	0.190	0.148	0.099
	R^2	0.611	0.682	0.792
	SSE	5.417	22.420	24.913

$\mathbf{Q_e}$ (mg/g) is the equilibrium adsorption.
k_1 (min^{-1}); k_2 (g/mg min); k_p (mg/g min$^{1/2}$); k_{fd} (min^{-1}) are the rate constant of the PFO, PSO, IPD, and LFD equation and.
C is a constant characteristic of boundary layer for IPD equation.
α (mg min^{-1}) is the initial removal rate.
β (g mg^{-1}) is a constant for surface coverage and activation energy.
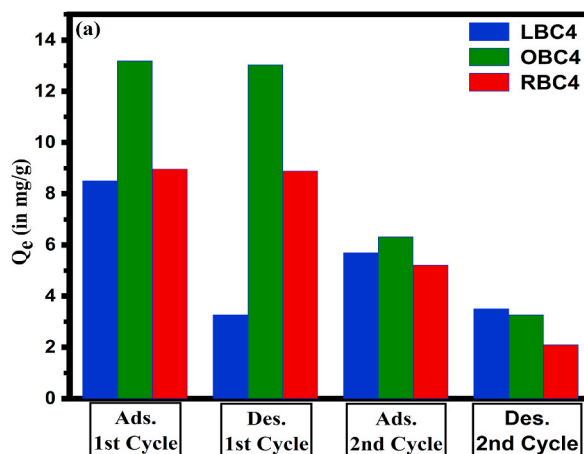
Fig. 7. Adsorption–desorption cycle performance for batch adsorption of Cr(VI) (0.1 g L^{-1}) at pH 3 onto L/O/RBC4 biochar and desorption using 1 M NaOH.

4. Cr(VI) adsorption mechanism

The FTIR and XPS analysis of the Cr(VI) adsorbed biochar reveals the reduction of Cr(VI) in presence of the biochar L/O/RBC4-6. However, the high pyrolysis temperature (PT) biochar (L/O/RBC6) show less Cr(VI) adsorption in comparison to lower PT biochar (L/O/RBC4). Thus, there is a significant role of the OFGs on biochar surface in Cr(VI) adsorption. Further it is observed that the OFGs undergo tremendous change in the O1 speak in XPS for biochar OBC4, which strengthens the role of oxygen functional groups in the Cr(VI) adsorption [71]. The OBC4 has more oxidized carboxylate functional moieties whereas RBC4 has reduced functional moieties, as evident from the XPS and FTIR studies. Thus, the reduction of RBC4 was expected to a greater extent than in case of OBC4. On the contrary, the results reveal OBC4 as the candidate with higher adsorption efficiency. This fact could be attributed to the ability of OBC4 to accommodate the reduced Cr(III) ions on its surface in comparison to the reduced biochar RBC4 [68]. Thus based on the above facts, the mechanism proposed for the adsorption of Cr(VI) onto biochar L/O/RBC4 is as depicted in Fig. 8. The alcoholic and phenolic moieties on all the modified biochar are reduced. Whereas the carbonyl and carboxylate moiety tends to bind and chelate the Cr(III) ion. Thus, as the OBC4 has more chelating functional groups apart from reducing phenol groups on the biochar, the Cr(VI) adsorption via reduction and chelation of Cr(III)is optimum in OBC4.

The adsorption of Cr(VI) by leached rice straw biochar (LBC4-6) is less than that depicted in Table 4. This could be attributed to the high ash content of rice straw and subsequently leached biochar obtained [42]. However, the Cr(VI) adsorption using oxidized and reduced biochar is found to be at par with other biochar reported in literature. Thus, by modification of rice straw biochar by oxidation and reduction of adsorbent with two-fold improvement in adsorption efficiency is obtained.
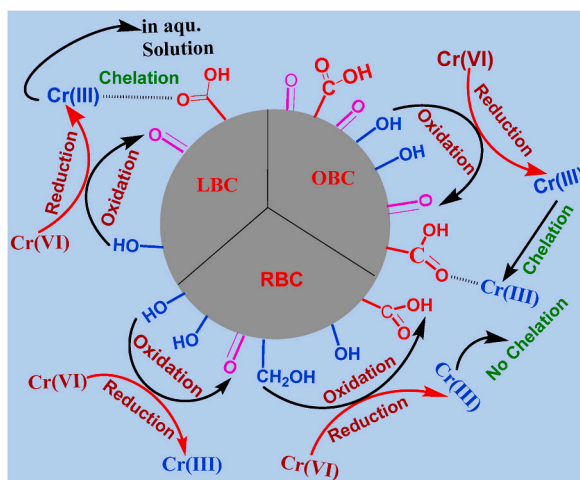

Fig. 8. Mechanism of Cr(VI) adsorption on the surface of leached, oxidized and reduced biochar (L/O/RBC4-6).

Table 4

Comparative study of adsorption capacities of various biochar with L/O/RBC4-6 for Cr(VI) Removal.

Adsorbent (Biochar)	Qe (mg/g)	References
Cherry biochar	16.01	[72]
Oleaster biochar	24.65	[72]
Wheat straw	24.60	[73]
Wicker biochar	23.60	[73]
Rice husk biochar	23.1	[74]
CTAB-Peanut Shell biochar	22.93	[75]
Peanut shell biochar	18.54	[75]
Cotton Stalk	15.56	[76]
Walnut shell	17.72	[76]
Hematite-modified biochar–clay granular	19.51	[77]
Ball-milled Fe^0 –biochar composite	14.59	[78]
Leached rice straw biochar (LBC4)	10.23	Present study
Oxidized biochar (OBC4)	17.47	Present study
Reduced biochar (RBC4)	15.27	Present study

5. Conclusion

Present study involving leached, oxidized and reduced biochar (L/O/RBC4-6) emphasized on the role of dynamic functional groups like lactones, carboxylate and phenolic apart from surface area and surface charge to have a considerable impact on the adsorption of the Cr(VI). The work establishes the mechanism of adsorption of Cr(VI) onto biochar to be reductive chelation on the surface of biochar. However, the reducing characteristics of modified biochar has no direct influence on the adsorption of Cr(VI) onto biochar. The oxygen functional groups (OFGs) with balance of both reducing characteristics and chelation of reduced chromium [Cr(III)] are essential for maximum efficiency of biochar/modified biochar. Cr(VI) adsorption using OFGs on biochar surface is quit complex and needs to be investigated for other appropriate functional group on biochar for Cr(VI) adsorption. The organic functional characteristics of biochar could affect the biochar capacity to adsorb Cr(VI) oxoanions and need further investigations for efficient adsorbents based on biochar.

6. Experimental section

6.1. Material

Acetic acid, hydrogen peroxide, K_2CrO_7, H_2SO_4, $KMnO_4$, 0.1 N HCl, 0.1 N NaOH, acetone, methanol and 2,4-diphenylcarbazide used for the studies are highest purity grade and purchased from Loba Chemie and utilised without further purification. All the reagents solution was prepared using deionized water.

6.2. Synthesis of oxidized (OBC4-6)

Rice straw biomass was collected from the agriculture field near the Bathinda city, Punjab, India. Air-dried the straw and chopped the straw to obtain the 1.18 mm sized using a sieve of equivalent mesh. The synthesis of adsorbents as biochar from rice straw at 400, 500 and 600 °C was performed in order to evaluate the characteristics and potential applications of the resulting materials. Rice straw was pyrolyzed in a muffle furnace at different temperatures 400 °C (BC4), 500 °C (BC5) or 600 °C (BC6) and a heating rate of 10 °C/min. The pyrolysis biochar BC4, BC5, or BC6 was subjected to acid leaching under TCLP condition [42]. Biochar was added to leachant (acetic acid with pH 2.8) in liquid–solid ratio of 20:1 (500 mL/25 g) in polythene bottles and shaking in an overhead shaker for 24 h. Further, the sample was filtered under vacuum to obtain the leached biochar (LBC4-6) respectively from biomass pyrolyzed biochar BC4–6 [42]. The leached biochar LBC4-6 were oven-dried at 105 ∓2 °C for 24 h and store in air tight lid plastic container. Oxidized biochar were synthesis by modified Hummer's method.

6.3. Reduced biochar (RBC4-6)

The reduced biochar (RBC4-6) were synthesize from the oxidized biochar, firstly by esterification of oxidized biochar (OBC4-6) using methanol/HCl followed by reduction with $NaBH_4/I_2$ suspension in THF (Scheme 1) [79]. The reaction was reflux for 5 h and subsequently the excess $NaBH_4$ was quenched by addition of methanol. The reduced biochar (RBC4-6) was obtained upon filtration of the suspension under vacuum and subsequently washing with deionized water.

6.4. Characterization of modified biochar

Leached biochar (LBC4-6), modified oxidized biochar (OBC4-6), and reduced biochar (RBC4-6) were characterized for pH using the pH meter (Model- PH 550 PH/mV/meter, OAKTON), ash content; surface morphology using CARL-ZEISS Merline Compact, functional groups using BRUKER TENSOR-27 Fourier Transform Infra-Red (FTIR) spectrometer, surface charge using Anton Paar XT-500

Zetasizer; elemental composition using ELEMENTAR, Model UNICUBE and X-ray photoelectron spectroscopy Model Thermoscientific NEXA. Surface area, pore volume, and pore size of biochar sample measure using Brunauer–Emmett–Teller (BET) equation with multipoint adsorption isotherm of N_2 at 77 K using a gas sorption analyser (BELSORP MAX analyser). The TCLP leached biochar were characterized and reported earlier [42], a comparative note would be addressed at relevant discussions.

6.5. Batch adsorption study

Batch adsorption studies were carried out at room temperature by dosing adsorbent at 0.1 g/L to a 100 mL Cr(VI) solution in Erlenmeyer flasks. The effect of pH (3–10), adsorbent dose (0.05–0.20 g/L), initial Cr(VI) concentration (2–10 mg/L) and contact time (0–24 h) were studied. For batch adsorption studies, to a 100 mL of Cr(VI) solution (2–10 mg/L) in the flask, pH maintained at 3 using 0.01 N HCl/NaOH solution and 10 mg of adsorbent (L/O/RBC4-6) was added. The flasks were kept in a rotary shaker at 180 ± 5 rpm for 24 h at 25 ± 2 °C. The batch samples were centrifuged at 7800 rpm for 15 min, supernatant was collected and analyzed for Cr(VI) concentration using 1,5-diphenylcarbazide method [61,80]. The equilibrium adsorption capacity (Q_e) and percentage removal (% R) of Cr(VI) were calculated using Eq. (8) and Eq. (9), respectively [13,81].

$$Q_e = \frac{(C_0 - C_e)V}{W} \tag{8}$$

$$\% R = \frac{C_0 - C_e}{C_0} \times 100 \tag{9}$$

where C_0 and C_e are the initial and final equilibrium concentration of Cr(VI) (in mg/L), V is the volume of solution taken (in L) and W is the amount of biochar used for adsorption (g).

For the kinetic studies, to a 10 mg/L aqueous Cr(VI) solution was added 0.10 g/L of adsorbent L/O/RBC4 maintained at pH 3 and shaken under 180 ±5 rpm at 25 ± 2 °C. The aliquot of the sample was taken at different time intervals and Cr(VI) analyzed.

6.6. Statistical analysis of adsorption isotherm and kinetics

MS-Excel with data Solver add-ins has been used to perform the nonlinear regression and error analysis for Cr(VI) adsorption. Sum of square error (SSE) minimization was used to do a nonlinear regression analysis of the adsorption equilibrium for the Langmuir, Freundlich, PFO, PSO, Elovich, IPD and LFD kinetics models (Eq. (10)).

$$SSE = \sum_{i=1}^{n} \left(Q_{i,model} - Q_{e,Exp} \right) \tag{10}$$

where SSE stand for Sum of square of error, $Q_{i, exp}$ and $Q_{i, model}$ represents the average of experimentally measured and predicted, experimentally measured Q values, respectively. n stand for the number of experimental points of fitted model.

CRediT authorship contribution statement

Amarjeet Dahiya: Writing – original draft, Methodology, Formal analysis, Data curation, Conceptualization. **Akanksha Bhardwaj:** Validation, Methodology, Formal analysis, Data curation. **Archana Rani:** Investigation, Formal analysis, Data curation. **Meenu Arora:** Writing – review & editing, Supervision, Project administration, Methodology. **J. Nagendra Babu:** Writing – review & editing, Supervision, Project administration, Conceptualization.

Declaration of competing interest

The authors declare the following financial interests/personal relationships which may be considered as potential competing interests:J NAGENDRA BABU AND MEENU ARORA reports financial support was provided by DSTWater technology Initiative, New Delhi.

Acknowledgements

Appendix A. Supplementary data

Supplementary data to this article can be found online at https://doi.org/10.1016/j.heliyon.2023.e21735.

References

[1] H. Li, X. Dong, E.B. da Silva, L.M. de Oliveira, Y. Chen, L.Q. Ma, Mechanisms of metal sorption by biochars: biochar characteristics and modifications, Chemosphere 178 (2017) 466–478, https://doi.org/10.1016/j.chemosphere.2017.03.072.

[2] A. Shakya, A. Núñez-Delgado, T. Agarwal, Biochar synthesis from sweet lime peel for hexavalent chromium remediation from aqueous solution, J. Environ. Manag. 251 (2019), 109570, https://doi.org/10.1016/j.jenvman.2019.109570.

[3] P. Sharma, V. Bihari, S.K. Agarwal, V. Verma, C.N. Kesavachandran, B.S. Pangtey, N. Mathur, K.P. Singh, M. Srivastava, S.K. Goel, Groundwater contaminated with hexavalent chromium [Cr (VI)]: a health survey and clinical examination of community inhabitants (Kanpur, India), PLoS One 7 (2012), e47877, https://doi.org/10.1371/journal.pone.0047877.

[4] M. Owlad, M.K. Aroua, W.A.W. Daud, S. Baroutian, Removal of hexavalent chromium-contaminated water and wastewater, A Review, Water Air Soil Pollut 200 (2009) 59–77, https://doi.org/10.1007/s11270-008-9893-7.

[5] J. Pan, J. Jiang, R. Xu, Removal of Cr(VI) from aqueous solutions by Na2SO3/FeSO4 combined with peanut straw biochar, Chemosphere 101 (2014) 71–76, https://doi.org/10.1016/j.chemosphere.2013.12.026.

[6] Z.-R. Guo, G. Zhang, J. Fang, X. Dou, Enhanced chromium recovery from tanning wastewater, J. Clean. Prod. 14 (2006) 75–79, https://doi.org/10.1016/j.jclepro.2005.01.005.

[7] A. Pérez-González, A.M. Urtiaga, R. Ibáñez, I. Ortiz, State of the art and review on the treatment technologies of water reverse osmosis concentrates, Water Res. 46 (2012) 267–283, https://doi.org/10.1016/j.watres.2011.10.046.

[8] A.K. Golder, A.N. Samanta, S. Ray, Removal of trivalent chromium by electrocoagulation, Separation and Purification Technology 53 (2007) 33–41, https://doi.org/10.1016/j.seppur.2006.06.010.

[9] A. Hafez, S. El-Mariharawy, Design and performance of the two-stage/two-pass RO membrane system for chromium removal from tannery wastewater. Part 3, Desalination 165 (2004) 141–151, https://doi.org/10.1016/j.desal.2004.06.016.

[10] P. Xie, Xiuli Hao, Osama Abdalla Mohamad, Jianqiang Liang, and Gehong Wei. "Comparative study of chromium biosorption by Mesorhizobium amorphae strain CCNWGS0123 in single and binary mixtures, Appl. Biochem. Biotechnol. 169 (2013) 570–587, https://doi.org/10.1007/s12010-012-9976-1.

[11] N.J. Durai, G.V.T. Gopala Krishna, V.C. Padmanaban, N. Selvaraju, Oxidative removal of stabilized landfill leachate by Fenton's process: process modeling, optimization & analysis of degraded products, RSC Adv. 10 (2020) 3916–3925, https://doi.org/10.1039/C9RA09415F.

[12] H. Jabeen, V. Chandra, S. Jung, J.W. Lee, K.S. Kim, S.B. Kim, Enhanced Cr(VI) removal using iron nanoparticle decorated graphene, Nanoscale 3 (2011) 3583–3585, https://doi.org/10.1039/C1NR10549C.

[13] T.C. Egbosiuba, A.S. Abdulkareem, A.S. Kovo, E.A. Afolabi, J.O. Tijani, W.D. Roos, Enhanced adsorption of As(V) and Mn(VII) from industrial wastewater using multi-walled carbon nanotubes and carboxylated multi-walled carbon nanotubes, Chemosphere 254 (2020), 126780, https://doi.org/10.1016/j.chemosphere.2020.126780.

[14] T.C. Egbosiuba, A.S. Abdulkareem, J.O. Tijani, J.I. Ani, V. Krikstolaityte, M. Srinivasan, A. Veksha, G. Lisak, Taguchi optimization design of diameter-controlled synthesis of multi walled carbon nanotubes for the adsorption of Pb(II) and Ni(II) from chemical industry wastewater, Chemosphere 266 (2021), 128937, https://doi.org/10.1016/j.chemosphere.2020.128937.

[15] A. Saravanan, P.S. Kumar, M. Govarthanan, C.S. George, S. Vaishnavi, B. Moulishwaran, S.P. Kumar, S. Jeevanantham, P.R. Yaashikaa, Adsorption characteristics of magnetic nanoparticles coated mixed fungal biomass for toxic Cr(VI) ions in aquatic environment, Chemosphere 267 (2021), 129226, https://doi.org/10.1016/j.chemosphere.2020.129226.

[16] S. Mittal, U. Vaid, G. Nabi Najar, J. Nagendra Babu, Removal of hexavalent chromium from aqueous solution: a comparative study of cone biomass of "Picea smithiana" and activated charcoal, Desalination Water Treat. 57 (2016) 11081–11095, https://doi.org/10.1080/19443994.2015.1038594.

[17] Y.C. Sharma, V. Srivastava, C.H. Weng, S.n. Upadhyay, Removal of Cr(VI) from wastewater by adsorption on iron nanoparticles, Can. J. Chem. Eng. 87 (2009) 921–929, https://doi.org/10.1002/cjce.20230.

[18] R. Wnetrzak, J.J. Leahy, Katarzyna W. Chojnacka, Agnieszka Saeid, etelvino Novotny, Lars Stoumann Jensen, and Witold Kwapinski. "Influence of pig manure biochar mineral content on Cr (III) sorption capacity, Journal of Chemical Technology & Biotechnology 89 (2014) 569–578, https://doi.org/10.1002/jctb.4159.

[19] Y. Fang, K. Yang, Y. Zhang, C. Peng, A. Robledo-Cabrera, A. López-Valdivieso, Highly surface activated carbon to remove Cr(VI) from aqueous solution with adsorbent recycling, Environ. Res. 197 (2021), 111151, https://doi.org/10.1016/j.envres.2021.111151.

[20] U. Vaid, Sunil Mittal, J. Nagendra Babu, Removal of hexavalent chromium from aqueous solution using biomass derived fly ash from Waste-to-Energy power plant, Desalination Water Treat. 52 (2014) 7845–7855, https://doi.org/10.1080/19443994.2013.833554.

[21] D. Woolf, James E. Amonette, F. Alayne Street-Perrott, Johannes Lehmann, Stephen Joseph, Sustainable biochar to mitigate global climate change, Nat. Commun. 1 (2010) 56, https://doi.org/10.1038/ncomms1053.

[22] B.H. Cheng, Raymond J. Zeng, Hong Jiang, Recent developments of post-modification of biochar for electrochemical energy storage, Bioresour. Technol. 246 (2017) 224–233, https://doi.org/10.1016/j.biortech.2017.07.060.

[23] L.L. Zhang, X.S. Zhao, Carbon-based materials as supercapacitor electrodes, Chem. Soc. Rev. 38 (2009) 2520–2531, https://doi.org/10.1039/B813846J.

[24] Y.Y. Ye, Ting-Ting Qian, Hong Jiang, Co-loaded N-doped biochar as a high-performance oxygen reduction reaction electro catalyst by combined pyrolysis of biomass, Ind. Eng. Chem. Res. 59 (2020) 15614–15623, https://doi.org/10.1021/acs.iecr.0c03104.

[25] H. Lu, W. Zhang, Y. Yang, X. Huang, S. Wang, R. Qiu, Relative distribution of Pb^{2+} sorption mechanisms by sludge-derived biochar, Water Res. 46 (2012) 854–862, https://doi.org/10.1016/j.watres.2011.11.058.

[26] W.-H. Chen, A.T. Hoang, S. Nižetić, A. Pandey, C.K. Cheng, R. Luque, H.C. Ong, S. Thomas, X.P. Nguyen, Biomass-derived biochar: from production to application in removing heavy metal-contaminated water, Process Saf. Environ. Protect. 160 (2022) 704–733, https://doi.org/10.1016/j.psep.2022.02.061.

[27] da Silva Medeiros, Deborah Cristina Crominski, Christopher Nzediegwu, Chelsea Benally, Selamawit Ashagre Messele, Jin-Hyeob Kwak, M. Anne Naeth, Ok Yong Sik, Scott X. Chang, Gamal El-Din Mohamed, Pristine and engineered biochar for the removal of contaminants co-existing in several types of industrial wastewaters: a critical review, Sci. Total Environ. 809 (2022) 151120, https://doi.org/10.1016/j.scitotenv.2021.151120.

[28] Y. Xiao, Lin Liu, Feifei han, and Xiuyun Liu. "Mechanism on Cr (VI) removal from aqueous solution by camphor branch biochar, Heliyon 8 (2022), https://doi.org/10.1016/j.heliyon.2022.e10328.

[29] N. Chen, S. Cao, L. Zhang, X. Peng, X. Wang, Z. Ai, L. Zhang, Structural dependent Cr(VI) adsorption and reduction of biochar: hydrochar versus pyrochar, Sci. Total Environ. 783 (2021), 147084, https://doi.org/10.1016/j.scitotenv.2021.147084.

[30] M.S. Rashid, G. Liu, B. Yousaf, Y. Hamid, A. Rehman, M. Arif, R. Ahmed, A. Ashraf, Y. Song, A critical review on biochar-assisted free radicals mediated redox reactions influencing transformation of potentially toxic metals: Occurrence, formation, and environmental applications, Environ. Pollut. 315 (2022), 120335, https://doi.org/10.1016/j.envpol.2022.120335.

[31] X. Dong, L.Q. Ma, J. Gress, W. Harris, Y. Li, Enhanced Cr(VI) reduction and As(III) oxidation in ice phase: important role of dissolved organic matter from biochar, J. Hazard Mater. 267 (2014) 62–70, https://doi.org/10.1016/j.jhazmat.2013.12.027.

[32] S. Chatzimichailidou, Maria Xanthopoulou, Athanasia K. Tolkou, Ioannis A. Katsoyiannis, Biochar derived from rice by-products for arsenic and chromium removal by adsorption: a review, Journal of Composites Science 7 (2023) 59, https://doi.org/10.3390/jcs7020059.

[33] S. Praveen, Josephraj Jegan, Thillainayagam Bhagavathi Pushpa, Ravindiran Gokulan, and Laura Bulgariu. "Biochar for removal of dyes in contaminated water: an overview, Biochar 4 (2022) 10, https://doi.org/10.1007/s42773-022-00131-8.

[34] Baiyan Zeng, Wenbin Xu, Sher Bahadar Khan, Yanjie Wang, Jing Zhang, Jiakuan Yang, Xintai Su, Lin Zhang, Preparation of sludge biochar rich in carboxyl/hydroxyl groups by quenching process and its excellent adsorption performance for Cr (VI), Chemosphere 285 (2021) 131439, https://doi.org/10.1016/j.chemosphere.2021.131439.

[35] W. Mao, L. Zhang, Y. Liu, T. Wang, Y. Bai, Y. Guan, Facile assembled N, S-co doped corn straw biochar loaded Bi$_2$WO$_6$ with the enhanced electron-rich feature for the efficient photocatalytic removal of ciprofloxacin and Cr(VI), Chemosphere 263 (2021), 127988, https://doi.org/10.1016/j.chemosphere.2020.127988.

[36] T. Masinga, M. Moyo, V.E. Pakade, Removal of hexavalent chromium by polyethyleneimine impregnated activated carbon: intra-particle diffusion, kinetics and isotherms, J. Mater. Res. Technol. 18 (2022) 1333–1344, https://doi.org/10.1016/j.jmrt.2022.03.062.

[37] M. Ahmadi, M. Foladivanda, N. Jaafarzadeh, Z. Ramezani, B. Ramavandi, S. Jorfi, B. Kakavandi, Synthesis of chitosan zero-valent iron nanoparticles-supported for cadmium removal: characterization, optimization and modeling approach, J. Water Supply Res. Technol. - Aqua 66 (2017) 116–130, https://doi.org/10.2166/aqua.2017.027.

[38] S. Tripathy, S. Sahu, R.K. Patel, R.B. Panda, P.K. Kar, Efficient removal of Cr(VI) by polyaniline modified biochar from date (Phoenix dactylifera) seed, Groundwater for Sustainable Development 15 (2021), 100653, https://doi.org/10.1016/j.gsd.2021.100653.

[39] N. Zhao, C. Zhao, K. Liu, W. Zhang, D.C.W. Tsang, Z. Yang, X. Yang, B. Yan, J.L. Morel, R. Qiu, Experimental and DFT investigation on N-functionalized biochars for enhanced removal of Cr(VI), Environ. Pollut. 291 (2021), 118244, https://doi.org/10.1016/j.envpol.2021.118244.

[40] M. Zhong, Li Meng, Bin Tan, Bin Gao, Yue Qiu, Xiaonan Wei, Hao Huiru, Zhixuan Xia, Qian Zhang, Investigations of Cr (VI) removal by millet bran biochar modified with inorganic compounds: Momentous role of additional lactate, Sci. Total Environ. 793 (2021), 148098, https://doi.org/10.1016/j.scitotenv.2021.148098.

[41] D.C. Marcano, Dmitry V. Kosynkin, Jacob M. Berlin, Sinitskii Alexander, Zhengzong Sun, Slesarev Alexander, Lawrence B. Alemany, Wei Lu, James M. Tour, Improved synthesis of graphene oxide, ACS Nano 4 (2010) 4806–4814, https://doi.org/10.1021/nn1006368.

[42] A. Bhardwaj, Shilpa Nag, Amarjeet Dahiya, Puneeta Pandey, Meenu Arora, and J. Nagendra Babu. "Effect of pyrolysis temperature on mechanistic transformation for adsorption of methylene blue on leached rice-straw biochar, CLEAN–Soil, Air, Water 50 (2022), 2100108, https://doi.org/10.1002/clen.202100108.

[43] S. Sadighian, Nahid Bayat, Sahar Najaflou, Mehraneh Kermanian, and Mehrdad Hamidi. "Preparation of graphene oxide/Fe3O4 nanocomposite as a potential magnetic nanocarrier and MRI contrast agent, ChemistrySelect 6 (2021) 2862–2868, https://doi.org/10.1002/slct.202100195.

[44] S. Sadighian, M. Abbasi, S.A. Arjmandi, H. Karami, Dye removal from water by zinc ferrite-graphene oxide nanocomposite, Progress in Color, Colorants and Coatings 11 (2018) 85–92, https://doi.org/10.30509/PCCC.2018.75743.

[45] A. Bhardwaj, Shilpa Nag, Khadim Hussain, Meenu Arora, Puneeta Pandey, J. Nagendra Babu, Adsorption of Zn (II) on pristine and SPLP/TCLP leached rice straw biochar: an interplay of precipitation and ion exchange, Water, Air, Soil Pollut. 233 (2022) 475, https://doi.org/10.1007/s11270-022-05940-y.

[46] A. Nawaz, B. Singh, P. Kumar, H3PO4-modified Lagerstroemia speciosa seed hull biochar for toxic Cr(VI) removal: isotherm, kinetics, and thermodynamic study, Biomass Conv. Bioref. 13 (2023) 7027–7041, https://doi.org/10.1007/s13399-021-01780-8.

[47] G.K. Gupta, Monoj Kumar Mondal, Mechanism of Cr (VI) uptake onto sagwan sawdust derived biochar and statistical optimization via response surface methodology, Biomass Conversion and Biorefinery 13 (2023) 709–725, https://doi.org/10.1007/s13399-020-01082-5.

[48] X. Zhang, P. Zhang, X. Yuan, Y. Li, L. Han, Effect of pyrolysis temperature and correlation analysis on the yield and physicochemical properties of crop residue biochar, Bioresour. Technol. 296 (2020), 122318, https://doi.org/10.1016/j.biortech.2019.122318.

[49] R. Singh, D.V. Naik, R.K. Dutta, P.K. Kanaujia, Biochars for the removal of naphthenic acids from water: a prospective approach towards remediation of petroleum refinery wastewater, J. Clean. Prod. 266 (2020), 121986, https://doi.org/10.1016/j.jclepro.2020.121986.

[50] Mengfan Hong, Limei Zhang, Zhongxin Tan, Qiaoyun Huang, Effect mechanism of biochar's zeta potential on farmland soil's cadmium immobilization, Environ. Sci. Pollut. Control Ser. 26 (2019) 19738–19748, https://doi.org/10.1007/s11356-019-05298-5.

[51] Oualid Abou, Hicham, Youness Abdellaoui, Laabd Mohamed, Mahmoud El Ouardi, Younes Brahmi, Iazza Mohamed, Jaouad Abou Oualid, Eco-efficient green seaweed codium decorticatum biosorbent for textile dyes: characterization, mechanism, recyclability, and RSM optimization, ACS Omega 5 (2020) 22192–22207, https://doi.org/10.1021/acsomega.0c02311.

[52] K. Rostamizadeh, Somayeh Rezaei, Majid Abdouss, Somayeh Sadighian, Saeed Arish, A hybrid modeling approach for optimization of PMAA–chitosan–PEG nanoparticles for oral insulin delivery, RSC Adv. 5 (2015) 69152–69160, https://doi.org/10.1039/C5RA07082A.

[53] K.S.W. Sing, R.T. Williams, The Use of Molecular Probes for the Characterization of Nanoporous Adsorbents, Particle & Particle Systems Characterization 21 (2004) 71–79, https://doi.org/10.1002/ppsc.200400923.

[54] J. Li, F. He, X. Shen, D. Hu, Q. Huang, Pyrolyzed fabrication of N/P co-doped biochars from (NH4)3PO4-pretreated coffee shells and appraisement for remedying aqueous Cr(VI) contaminants, Bioresour. Technol. 315 (2020), 123840, https://doi.org/10.1016/j.biortech.2020.123840.

[55] Del Bubba, Massimo, Beatrice Anichini, Zaineb Bakari, Maria Concetta Bruzzoniti, Roberto Camisa, Claudia Caprini, Leonardo Checchini, et al., Physicochemical properties and sorption capacities of sawdust-based biochars and commercial activated carbons towards ethoxylated alkyl phenols and their phenolic metabolites in effluent wastewater from a textile district, Sci. Total Environ. 708 (2020), 135217, https://doi.org/10.1016/j.scitotenv.2019.135217.

[56] X. Xu, Huang Huang, Yue Zhang, Zibo Xu, Xinde Cao, Biochar as both electron donor and electron shuttle for the reduction transformation of Cr (VI) during its sorption, Environ. Pollut. 244 (2019) 423–430, https://doi.org/10.1016/j.envpol.2018.10.068.

[57] Y. Chen, B. Wang, J. Xin, P. Sun, D. Wu, Adsorption behavior and mechanism of Cr(VI) by modified biochar derived from Enteromorpha prolifera, Ecotoxicol. Environ. Saf. 164 (2018) 440–447, https://doi.org/10.1016/j.ecoenv.2018.08.024.

[58] Y. Li, X. Chen, L. Liu, P. Liu, Z. Zhou, Huhetaoli, Y. Wu, T. Lei, Characteristics and adsorption of Cr(VI) of biochar pyrolyzed from landfill leachate sludge, J. Anal. Appl. Pyrol. 162 (2022), 105449, https://doi.org/10.1016/j.jaap.2022.105449.

[59] A. Kumari Sharma, Rupesh S. Devan, Meenu Arora, Rabindra Kumar, Yuan-Ron Ma, J. Nagendra Babu, Reductive-co-precipitated cellulose immobilized zerovalent iron nanoparticles in ionic liquid/water for Cr (VI) adsorption, Cellulose 25 (2018) 5259–5275, https://doi.org/10.1007/s10570-018-1932-y.

[60] Z. Wu, H. Zhong, X. Yuan, H. Wang, L. Wang, X. Chen, G. Zeng, Y. Wu, Adsorptive removal of methylene blue by rhamnolipid-functionalized graphene oxide from wastewater, Water Res. 67 (2014) 330–344, https://doi.org/10.1016/j.watres.2014.09.026.

[61] S. Kumar, Ravinderdeep Singh Brar, J. Nagendra Babu, Amarjeet Dahiya, Sandip Saha, and Avneesh Kumar. "Synergistic effect of pistachio shell powder and nano-zerovalent copper for chromium remediation from aqueous solution, Environ. Sci. Pollut. Control Ser. 28 (2021) 63422–63436, https://doi.org/10.1007/s11356-021-15285-4.

[62] S. Biswas, Tushar Kanti Sen, Anteneh Mesfin Yeneneh, and Bhim Charan Meikap. "Synthesis and characterization of a novel Ca-alginate-biochar composite as efficient zinc (Zn2+) adsorbent: thermodynamics, process design, mass transfer and isotherm modeling, Separ. Sci. Technol. 54 (2019) 1106–1124, https://doi.org/10.1080/01496395.2018.1527353.

[63] Irving Langmuir, The adsorption of gases on plane surfaces of glass, mica and platinum, J. Am. Chem. Soc. 40 (1918) 1361–1403, https://doi.org/10.1021/ja02242a004.

[64] H.M.F. Freundlich, Uber die adsorption in Iosungen Zeitschrift fur physikalische Chemie (Leipzig) 57A (1906) 385–470, https://doi.org/10.1515/ZPCH-1907-5723.

[65] R. Yadav, A.K. Sharma, J.N. Babu, Sorptive removal of arsenite [As(III)] and arsenate [As(V)] by fuller's earth immobilized nanoscale zero-valent iron nanoparticles (F-nZVI): effect of Fe0 loading on adsorption activity, J. Environ. Chem. Eng. 4 (2016) 681–694, https://doi.org/10.1016/j.jece.2015.12.019.

[66] E.D. Revellame, D.L. Fortela, W. Sharp, R. Hernandez, M.E. Zappi, Adsorption kinetic modeling using pseudo-first order and pseudo-second order rate laws: a Review, Cleaner Engineering and Technology 1 (2020), 100032, https://doi.org/10.1016/j.clet.2020.100032.

[67] R. Verma, P.K. Maji, S. Sarkar, Comprehensive investigation of the mechanism for Cr(VI) removal from contaminated water using coconut husk as a biosorbent, J. Clean. Prod. 314 (2021), 128117, https://doi.org/10.1016/j.jclepro.2021.128117.

[68] H. Wang, W. Wang, X. Gao, Adsorption Mechanism of Cr(VI) on Woody Activated Carbons, 2022, https://doi.org/10.2139/ssrn.4253338.

[69] S.J. Peighambardoust, R. Foroutan, S.H. Peighambardoust, H. Khatooni, B. Ramavandi, Decoration of Citrus limon wood carbon with Fe3O4 to enhanced Cd2+ removal: a reclaimable and magnetic nanocomposite, Chemosphere 282 (2021), 131088, https://doi.org/10.1016/j.chemosphere.2021.131088.

[70] F.C. Wu, R.L. Tseng, R.-S. Juang, Characteristics of Elovich equation used for the analysis of adsorption kinetics in dye-chitosan systems, Chem. Eng. J. 150 (2009) 366–373, https://doi.org/10.1016/j.cej.2009.01.014.

[71] X. Dong, L.Q. Ma, Y. Li, Characteristics and mechanisms of hexavalent chromium removal by biochar from sugar beet tailing, J. Hazard Mater. 190 (2011) 909–915, https://doi.org/10.1016/j.jhazmat.2011.04.008.

[72] H.T. Kahraman, E. Pehlivan, Cr6+ removal using oleaster (Elaeagnus) seed and cherry (Prunus avium) stone biochar, Powder Technol. 306 (2017) 61–67, https://doi.org/10.1016/j.powtec.2016.10.050.

[73] Aleksandra Tytlak, Patryk Oleszczuk, Ryszard Dobrowolski, Sorption and desorption of Cr (VI) ions from water by biochars in different environmental conditions, Environ. Sci. Pollut. Control Ser. 22 (2015) 5985–5994, https://doi.org/10.1007/s11356-014-3752-4.

[74] Y. Ma, W.-J. Liu, N. Zhang, Y.-S. Li, H. Jiang, G.-P. Sheng, Polyethylenimine modified biochar adsorbent for hexavalent chromium removal from the aqueous solution, Bioresour. Technol. 169 (2014) 403–408, https://doi.org/10.1016/j.biortech.2014.07.014.

[75] H.A. Murad, M. Ahmad, J. Bundschuh, Y. Hashimoto, M. Zhang, B. Sarkar, Y.S. Ok, A remediation approach to chromium-contaminated water and soil using engineered biochar derived from peanut shell, Environ. Res. 204 (2022) 112125, https://doi.org/10.1016/j.envres.2021.112125.

[76] J. Wan, F. Liu, G. Wang, W. Liang, C. Peng, W. Zhang, K. Lin, J. Yang, Exploring different mechanisms of biochars in removing hexavalent chromium: sorption, reduction and electron shuttle, Bioresour. Technol. 337 (2021), 125382, https://doi.org/10.1016/j.biortech.2021.125382.

[77] S. Zhu, S. Wang, X. Yang, S. Tufail, C. Chen, X. Wang, J. Shang, Green sustainable and highly efficient hematite nanoparticles modified biochar-clay granular composite for Cr(VI) removal and related mechanism, J. Clean. Prod. 276 (2020), 123009, https://doi.org/10.1016/j.jclepro.2020.123009.

[78] K. Wang, Y. Sun, J. Tang, J. He, H. Sun, Aqueous Cr(VI) removal by a novel ball milled Fe0-biochar composite: role of biochar electron transfer capacity under high pyrolysis temperature, Chemosphere 241 (2020), 125044, https://doi.org/10.1016/j.chemosphere.2019.125044.

[79] J.N. Babu, V. Bhalla, M. Kumar, R.K. Puri, R.K. Mahajan, Chloride ion recognition using thiourea/urea based receptors incorporated into 1,3-disubstituted calix [4] arenes, New J. Chem. 33 (2009) 675–681, https://doi.org/10.1039/B816610B.

[80] A. Lace, D. Ryan, M. Bowkett, J. Cleary, Chromium monitoring in water by colorimetry using Optimised 1,5-diphenylcarbazide method, Int. J. Environ. Res. Publ. Health 16 (2019) 1803, https://doi.org/10.3390/ijerph16101803.

[81] T.C. Egbosiuba, Michael chika egwunyenga, Jimoh Oladejo Tijani, Saheed Mustapha, Ambali Saka Abdulkareem, Abdulsalami Sanni Kovo, Vida Krikstolaityte, Andrei Veksha, Michal Wagner, and Grzegorz Lisak. "Activated multi-walled carbon nanotubes decorated with zero valent nickel nanoparticles for arsenic, cadmium and lead adsorption from wastewater in a batch and continuous flow modes, J. Hazard Mater. 423 (2022), 126993, https://doi.org/10.1016/j.jhazmat.2021.126993.